

Swift UVOT

MULLARD SPACE SCIENCE LABORATORY
UNIVERSITY COLLEGE LONDON

Author: H. Kawakami

Life time performance of FM-intensifier in analog mode

Document Number: Swift-UVOT/MSSL/TC/00???.01

17-July-00

Distribution:

TN004-01

270 chos

Swift-UVOT Project Office

T Kennedy

Orig.

Mullard Space Science Laboratory

K Mason
A Smith
B Hancock
H Kawakami

DEP

17 July 2000
Hajime Kawakami

Life time performance of FM-intensifier in analog mode

1. Introduction

The previous report (Swift-UVOT/MSSL.TC/0002) showed capability of analog mode for high time resolution photometry, when a target star was brighter than 17.4mag. Swift UVOT may have several bright stars in the field of view during monitoring time variation of a gamma ray burster. It is dangerous for the intensifier to observe a bright star for a long time in photon counting mode (high gain in MCPs). The analog mode observation will offer the longer life time, since the electric gain of MCPs is less than 1/6 of the photon counting mode.

Quantifying very bright star as a stand alone system is one of the safety requirements for Swift UVOT. Analog mode is one of the candidate to fulfil this requirement. It is, however, essential to know, how long does the detector withstand against the intense star illumination during the brightness assessment.

Our intensified CCD detector demonstrated far longer life time (>100 times) than typical position sensitive detectors in terms of accumulated anode charge (XMM-OM/MSSL/TC/0059). This difference may be due to the lower gain of MCPs with our detector, i.e. $\sim 5 \times 10^5$ with ours while $\sim 10^7$ with the position sensitive detectors. If the life time depends on the gain strongly, the reduction of the gain by the factor of 6 may extend the life time far longer than x6.

In this report, the image intensifier was operated in the analog mode and was exposed to intense pinhole illuminations for 100 hours. Gain depletion of MCPs and sensitivity loss in F-F images were investigated against accumulated charge.

2. Electric gain

The best result in analog mode was obtained with 90% of nominal photon counting MCP voltage in the test with DEP_#5 intensifier. The experiments in this report was carried out with DEP_#8 intensifier, whose nominal MCPs voltage is 2250V. The 2020V, 90% of the nominal, was applied to the MCPs during the photon dose. The illumination pattern was a 11x11 pinhole array and the brightness has gradient along the column in the dynamic range of $\sim 2 \times 10^4$ (Fig. 1). The light source is made of 64 green LEDs covered with a diffuser and a 5300-5700Å interference filter. The brightness of the LEDs is controlled by a constant current source in the dynamic range of $\sim 2 \times 10^4$ (see detail in XMM-OM/MSSL.TC/0057).

The brightness of the pinhole array was calibrated with 3 photon counting images in the 3 LED current levels, L=1, L=3 and L=10 in order to overcome small dynamic range of the

detector. The lower LED current (L=1) was used for determining brightness ratio among bright pinhole columns, while the medium LED current (L=3) was for faint pinhole columns (Table 1). The highest current (L=10) was for the calibration of LED brightness during the photon dose, in which the faintest pinhole column (col=1) still gave useful data. Photon losses due to coincidence were corrected and the true input rates were tabulated in Table 2. Finally, the absolute brightness of the pinhole columns at the LED current level of L=10 was tabulated in Table 3.

Table 1. Raw counts /(hour x spot) 21 June 2000 DEP_#8

	LED = 1	3	10
col=11	264920.0	N/A	N/A
col=10	254720.0	N/A	N/A
col=9	32620.0	N/A	N/A
col=8	24460.0	N/A	N/A
col=7	2381.2	N/A	N/A
col=6	2131.9	23104.0	N/A
col=5	158.2	1680.4	N/A
col=4	84.1	1042.4	N/A
col=3	22.5	186.2	N/A
col=2	(7.0)	169.0	(253160.0)
col=1	14.2	164.6	264110.0

Table 2. True counts /(sec x spot) 21 June 2000 DEP_#8

	LED = 1	3	10
col=11	94.58122		
col=10	90.11536		
col=9	9.74329		
col=8	7.26678		
col=7	.69737		
col=6	.62426	6.85783	
col=5	.04627	.49191	
col=4	.02459	.30502	
col=3	.00658	.05446	
col=2	(.00205)	.04942	(89.43997)
col=1	.00415	.04814	94.22338

Table 3. Pinhole brightness at LED current level = 10

column	1	2	3	4	5	6	7	8	9	10	11
Brtness (c/s)	94.22	96.73	106.59	597.0	962.8	13.4k	15.0k	156k	209k	1938k	2034k
B0 star (mag)	16.5	16.5	16.4	14.5	14.0	11.1	11.0	8.4	8.1	5.7	5.6

The ratio of gains between $V_{mcp}=2250V$ (photon counting) and $2020V$ (analog) were determined from both of the brightness of event splash at phosphor screen and anode current. The pulse height distributions of the event splash with the 2 different voltages to MCPs were shown in Fig. 2. Flat filed in the count rate of 15,000 c/(sec full area) were used for the illumination. The brief ratio was determined from the peak positions, > 5.5 times. It was difficult to determine the ratio accurately, because the pulse height distribution with $V_{mcp}=2020V$ was squashed to the lower energy end.

The brighter F-F illumination was used for the measurement of the anode current to produce sufficient current with $V_{mcp}=2020V$. The detected count rate for the F-F was 86,100 c/(sec full area) in photon counting mode. After the correction of the coincidence loss, the true incoming rate was turned out to be 94,000 c/(sec full area). The procedure of the coincidence correction followed XMM-OM/MSSL.TC/0050. Coincidence area of event splashes was assumed to be $12 (CCD_pixels)^2$ from other 2 intensifiers, though there was no data on DEP_#8 itself. The full detector area in the photon counting imaging is $(3.37 \times 256 CCD_pixels)^2$, while photocathode area is circle with the diameter of 25mm. Since the anode current was produced from all photocathode area, incoming rate of electrons involved in anode current was $94,000 c/s * (D=25mm) / (3.37 \times 256 (CCD_pixels)^2 = 94,000 c/s * 1.2467 = 117,000 c/s$. A 99.91k Ohm resistor was inserted at the anode cable, whose voltage was at 8000V, and the small voltage drop across the resistor was measured with a precision multimeter, FLUKE 87 IV, in the minimum readout of 1uV. The resistance value was also calibrated by the FLUKE 87 IV. The small voltage drops were 1012uV and 151uV with $V_{mcp}=2250V$ and $2020V$. Hence, the currents were 10.23nA and 1.53nA. Since the input impedance of Fluke 87IV was 10M Ohm, anode currents were corrected by the factor of 1.01. Finally, the electric gain was calculated to be 5.4×10^5 with $V_{mcp}=2250V$ and 8.1×10^4 with $V_{mcp}=2020V$. The ratio of the gains with the 2 voltages was x6.7 times.

The electric gain in the high input rate was measured using pinhole illuminations in the LED current levels of L=1-10 for $V_{mcp}=2250V$ and L=3-10 for $V_{mcp}=2020V$. Columns=1-9 of the pinhole array was blocked for this measurement, so that the brightest 2 columns=10-11 with nearly same brightness were used for the illumination. Since voltage display of the FLUKE 87 IV was not stable in the last 2 digits (10uV, 1uV), the display was read 10 times and was averaged for the lowest 2 illuminations (i.e. LED current levels L=3 and L=4 for $V_{mcp}=2020V$ and L=1 and L=2 for $V_{mcp}=2250V$). The results for the both of $V_{mcp}=2250V$ and $V_{mcp}=2020V$ were tabulated in Table 4 and were plotted in Figs. 3 and 4. The electric gain of the intensifier was $5.7E+5$ in the

low input rate with $V_{mcp} = 2250V$ and $8.1E+4$ with $V_{mcp} = 2020V$. The gain depletion is $1/9.7$ in the input rate of $2E+6$ c/s with $V_{mcp} = 2250V$, while $1/8$ with $V_{mcp} = 2020V$, compared with those at the input rate of 100 c/s. The electric gains of pinhole illumination in the low input rate was higher than that of F-F illumination. This was due to global gain variation of MCPs (i.e. the local gain at pinhole positions were higher than the average).

Electric gain of MCPs at pinhole positions should have changed during the photon dose. The anode current was measured after completing the 100 hours photon dose by illuminating exactly same positions. This gauges the level of the change before and after the photon dose. Again, columns=1-9 of the pinhole array was blocked for the measurement, so that the brightest 2×11 pinholes from columns=10-11 were used for the illumination. The gains at the brightest pinhole positions at different input rate were tabulated in Table 5 and were plotted in Figs. 3 and 4 overlaying on the original gains. In spite of the large gain loss in the low input rate, the gain in the high input rate does not change before and after the 100 hours dose. This is particularly true for the illumination above $1E+5$ c/(sec x spot) with $V_{mcp} = 2250V$ and $1E+6$ c/(sec x spot) with $V_{mcp} = 2020V$. From these results, we can assume anode currents at columns=10 and 11 were constant throughout the photon dose, hence we can estimate total accumulated charge precisely. There is no measurement on the change of gain at other pinhole positions, i.e. columns=1-9. Since the total accumulated charges are smaller, the anode currents hopefully did not change much before and after the photon dose.

Because of the large gain loss in the low input rate while no gain loss in the high input rate after the 100 hours photon dose, the gradient of the gain curve against input rate becomes flat. This suggests a very hard scrubbing may lighten the effect of pore paralysis, hence may extend dynamic range of MCPs.

Table 4. Electric gain of XMM-OM tube in high count rate

LED Intensity (c/s pinhole)	Anode current (pA) from 22 pinholes		Electric Gain	
	2020V	2250V	2020V	2250V
F-F 94000	1530	10230	8.1 E+4	5.4 E+5
L=1 92.35	(6.7)	184	(2. E+4)	5.7 E+5
L=2 352	132	585	10. E+4	4.7 E+5
L=3 1014	295	1370	8.3 E+4	3.8 E+5
L=4 3426	800	2880	6.6 E+4	2.4 E+5
L=5 16500	2330	9260	4.0 E+4	1.6 E+5
L=6 51000	5250	20200	2.9 E+4	1.1 E+5
L=7 139000	11100	43300	2.3 E+4	0.88E+5
L=8 410000	29700	114000	2.1 E+4	0.79E+5
L=9 984000	57800	225000	1.7 E+4	0.65E+5
L=10 1986000	102000	412000	1.5 E+4	0.59E+5

20K \rightarrow 1.4E5

Table 5. Electric gain after 100 hours dose

LED Intensity (c/s pinhole)	Anode current (pA) from 22 pinholes		Electric Gain	
	2020V	2250V	2020V	2250V
L=1 92.35	---	64	---	2.0 E+5
L=2 352	---	219	---	1.8 E+5
L=3 1014	103	664	3. E+4	1.9 E+5
L=4 3426	239	1810	2. E+4	1.5 E+5
L=5 16500	1041	6550	1.8 E+4	1.1 E+5
L=6 51000	2790	16900	1.6 E+4	0.94E+5
L=7 139000	7700	38400	1.6 E+4	0.78E+5
L=8 410000	24000	108000	1.6 E+4	0.75E+5
L=9 984000	50200	225000	1.4 E+4	0.65E+5
L=10 1986000	94100	419000	1.3 E+4	0.60E+5

Ref-2 Files used in this section

/swift/ZPHD010.dat

ZPIN011.dat,ZPIN012.dat,ZPIN013.dat,ZPIN014.dat

3. Gain loss of MCPs

A reference pulse height distributions for individual pinhole columns, col=4-11 (600-2E+6 c/s), were measured with $V_{mcp}=2250V$ (photon counting mode) before starting the photon dose. The photon doses were carried out 3 times for 15 hours, 15 hours and 70 hours with $V_{mcp}=2020V$. The pulse height distributions were measured after the each photon dose. Fig. 5 shows the reference pulse height distribution and the one after the 100 hours dose by the 2E+6 c/s pinholes.

The gain reduced to 1/2.5 of the beginning. The gain loss was quantified from peak positions of the pulse height distributions. The gains after each dose were tabulated in Table 6, and were plotted against accumulated charge in Fig 6. Fig. 7 is the extract from XMM-OM/MSSL.TC/ 0059, in which the intensifier was operated in photon counting mode during the photon dose. The plots in analog mode coincides with those in photon counting mode. This implies that the gain loss can be described by the single parameter, **accumulated charge**, in any condition (i.e. different gain, input count rate, exposure time etc.).

Table 6. Gain depletion of MCPs

Dose time	Pinhole intensity (counts/sec)							
	2030k	1940k	210k	160k	15k	13k	960	600
15.0 hr	.623	.609	.735	.816	.890	.884	.907	.941
30.0 hr	.570	.573	.772	.807	.884	.862	.922	.916
100.0 hr	.363	.346	.589	.570	.793	.811	.924	.955

Ref-3 Files used in this section

/swift/ZPHD016.dat,ZPHD028.dat,ZPHD047.dat,ZPHD064.dat

4. Sensitivity loss in photon counting image

A reference F-F image with the blue (460nm) LED illumination was integrated for 15 hours in photon counting mode before starting the photon dose. F-F image integrations were followed after each intense illumination to see the sensitivity losses in the different level of dose. The integrations started after the sufficient period since the end of the intense illumination in order to avoid fluorescence, i.e. 80 hours in the 1st day, 38 hours the 2nd day and 27 hours the last day.

Fig. 8 shows 4 F-F images, one was taken prior to the photon dose for reference and the other 3 were after 15, 30 and 100 hours dose. The F-F after 100 hours dose clearly showed an array of black spots corresponding to the pinhole positions.

A F-F image in each day of photon dose was divided by the reference F-F to remove detector artefacts and illumination non-uniformity. Then, the 11x11 array of black spots were averaged along the columns to improve S/N. Central positions of the black spots coincided with the pinhole positions in the accuracy of 8 μ m along H_intensifier direction (bias direction of the 1st MCP), while systematically shifted by 15 μ m along V_intensifier direction. The day by day growth of the black spots is shown in Fig. 9. The image contains all factors, i.e. fluorescence, gain depletion and photocathode sensitivity loss. Fig. 10 shows profiles of the averaged black spots in the last day. Y-width of the slice is 3 twixel (= 58 μ m). The depth of black spots reached 25% at the brightest pinhole after 100 hours dose. The black spots were noticeable for the illumination intensities of > 13kc/s after 100 hours dose, but not for the lower intensity illuminations. Since the F-F integrations were started after the sufficiently long period since the end of the photon dose, the peak depths were only little affected by fluorescence (less than 1.4%).

The 6-10 dark frames were acquired in photon counting mode before and after the F-F integrations in order to correct the effect of fluorescence for further precision. Standard fluorescence profiles are shown in the lower panel of Fig. 9. The size of the fluorescence is far larger than both of the black spots and projected pinhole, i.e. from 220 μ m to 270 μ m. The fluorescence spots have offset from the pinhole positions by 200-240 μ m along H_intensifier direction (bias direction of the 1st MCP). The fluorescence spot got doughnut shape (i.e. black spot in central part) with the increase of the dose level. The details of these characteristics were identical to those described in the former report, XMM-OM/MSSL/TC/0057.

The sensitivity loss at the peak position was quantified from the average of 3x3 twixels square centred on the black spots. The normalization level was determined from 37x37 twixels (=717 μ m) square excluding central D=21 twixels circular area. Then, the effect of fluorescence (1.4 in maximum) was subtracted. The results were tabulated in Table 7 and were plotted against accumulated charge in Fig. 11. The sensitivity did not decrease till 1E-5 coulombs/spot. It started to decrease steeply from 1E-4 coulombs/spot.

The sensitivity loss seen in F-F image is the combination of gain depletion and photocathode sensitivity loss. The photocathode sensitivity losses were calculated by removing the effect of gain depletion (threshold=15ADU). The results were tabulated in Table 8 and were shown in Fig. 12. The sensitivity loss of photocathode is not noticeable up to 3E-5 coulombs/spot.

The photocathode sensitivity loss for the same intensifier but dosed in photon counting mode was extracted from XMM-OM/MSSL/TC/0057 (Fig. 13). The sensitivity loss dosed in analog mode shows slightly faster decrease above 2E-4 coulombs/spot. This result did not imply that ion barrier characteristics of the 1st MCP improved with the lower voltage.

A Gaussian profile was fitted to the black spots to quantify the spatial extent. The results are shown in Fig. 14. There are clear correlation with accumulated charge. The width increased from 80 μ m(FWHM) to 110 μ m after acquiring 1E-5 to 2E-3 coulombs/spot.

Table 7. Sensitivity change in blue F-F image at peak position

Dose time	Pinhole intensity (counts/sec)									
	2030k	1940k	210k	160k	15k	13k	960	600	110	97
15.0 hr	.933	.942	1.000	.993	1.002	1.010	1.006	1.001	.999	.984
30.0 hr	.864	.892	.971	.958	.979	.995	.994	1.002	1.000	1.001
100.0 hr	.743	.755	.907	.910	.956	.977	.997	.999	1.001	.997

Table 8. Photocathode sensitivity change at peak position

Dose time	Pinhole intensity (counts/sec)									
	2030k	1940k	210k	160k	15k	13k	960	600	110	97
15.0 hr	.951	.965	1.032	1.009	1.007	1.016	1.014	1.006	.999	.984
30.0 hr	.886	.917	.994	.975	.985	1.001	1.001	1.009	1.000	1.001
100.0 hr	.801	.823	.955	.950	.966	.983	1.004	1.003	1.001	.997

Ref-4 Files used in this section

/swift/ZDEP015.dat,ZDEP030.dat,ZDEP043.dat,ZDEP060.dat
 ZPHD016.dat,ZPHD028.dat,ZPHD047.dat,ZPHD064.dat
 ZDRK019.dat,ZDRK020.dat,ZDRK021.dat,ZDRK029.dat,ZDRK031.dat
 ZDRK032.dat
 ZDRK033.dat,ZDRK034.dat,ZDRK035.dat,ZPHD036.dat,ZPHD037.dat
 ZDRK038.dat,ZDRK039.dat,ZDRK042.dat,ZPHD044.dat,ZPHD045.dat
 ZDRK048.dat,ZDRK049.dat,ZDRK050.dat,ZPHD051.dat,ZPHD052.dat
 ZDRK053.dat,ZDRK054.dat,ZDRK055.dat,ZPHD059.dat,ZPHD061.dat

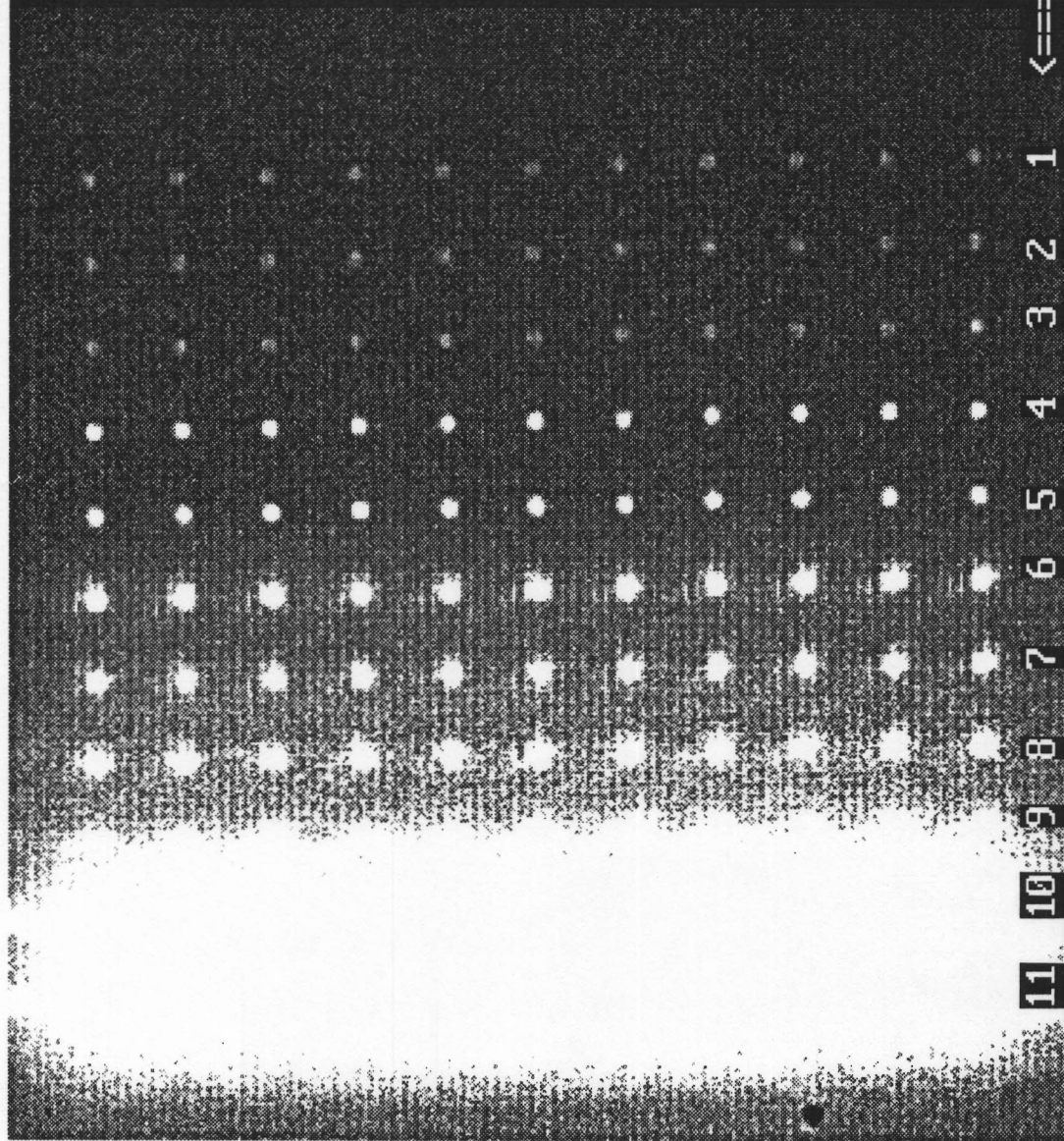
5. Summary

i) Gain loss dosed in analog mode was same as that in photon counting mode in terms of accumulated anode charge.

ii) Photocathode sensitivity loss dosed in analog mode was slightly faster (by ~30%) than that in photon counting mode in terms of accumulated anode charge.

iii) Gain loss measured in the low input rate was 1/2 - 1/3 after 100 hours photon dose, while that in the high input rate almost nothing. In the consequence, pore paralysis curve was flatten after the dose. This suggests a possibility of extending dynamic range of MCPs by a hard scrubbing.

Extract of 800x800 pixels
out of 2048x2048 full area



11 10 9 8 7 6 5 4 3 2 1 <==== Column

<----- 800 Subpixels ----->

Fig. 1 Pinhole array projected on the detector

10H 17M 16S 11H 17M 16S 2000/06/21/
Pin012 Calib L1 3600S 400-2250-5370 Cst=(65,95)100V (1624,456) D_#8

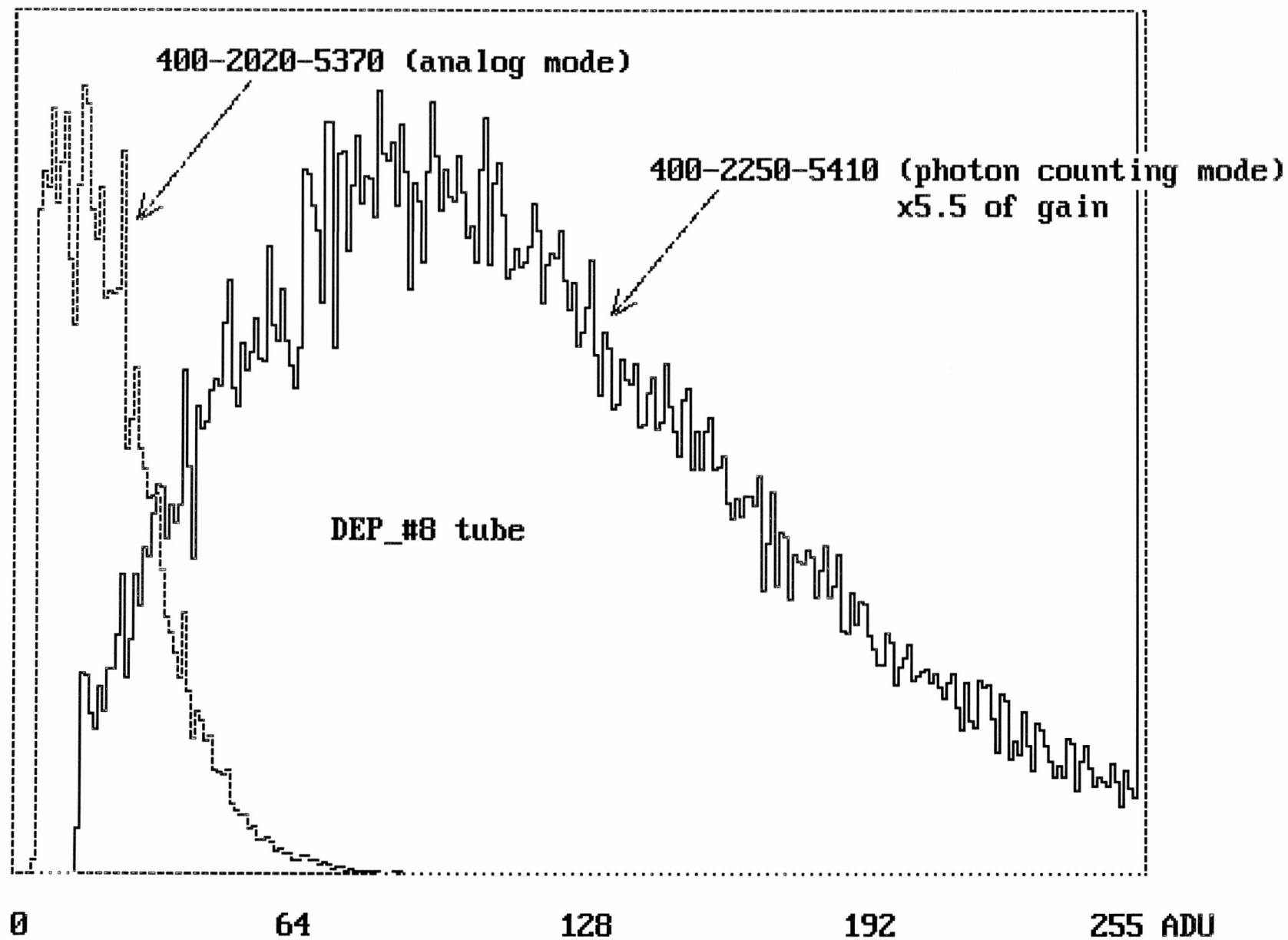
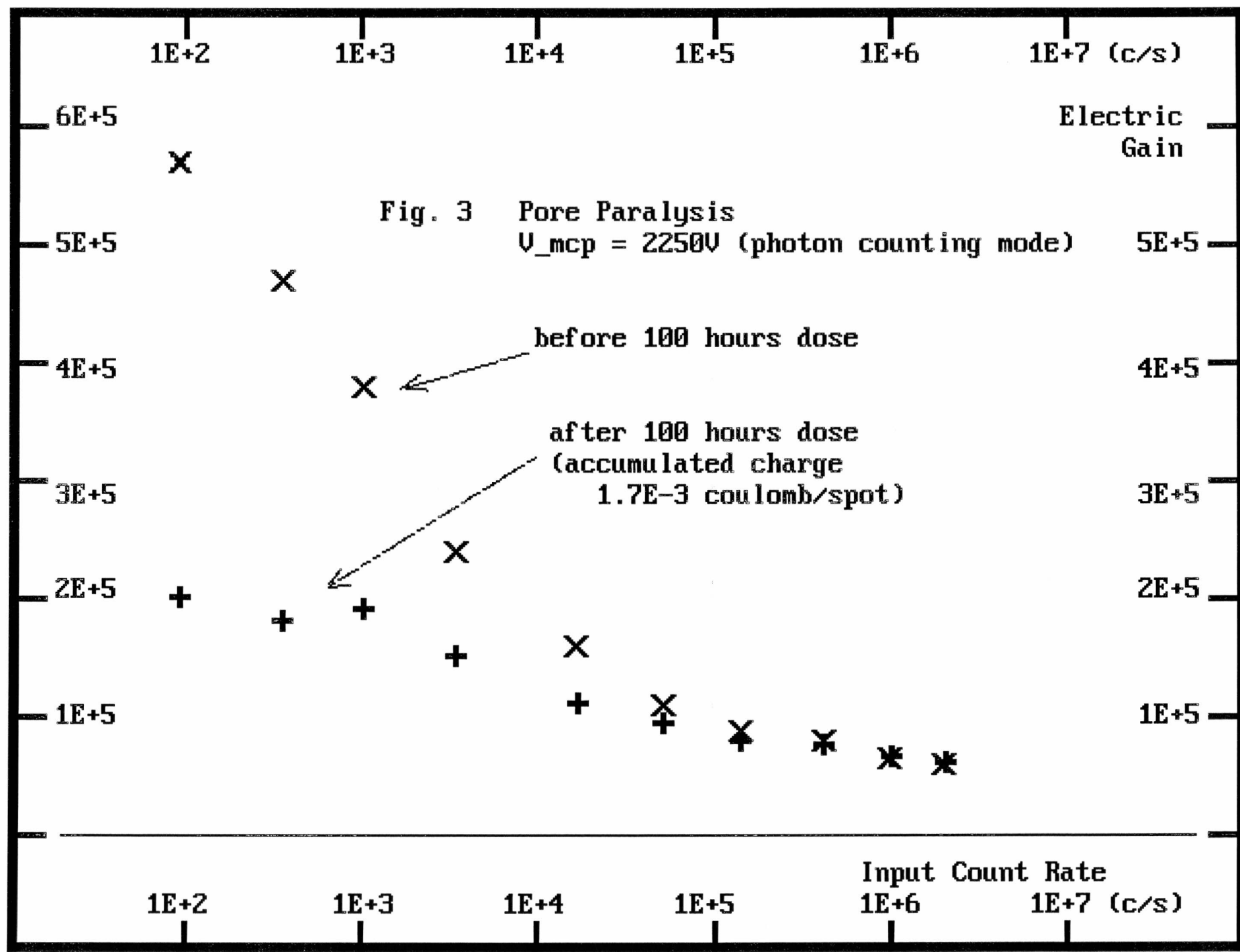
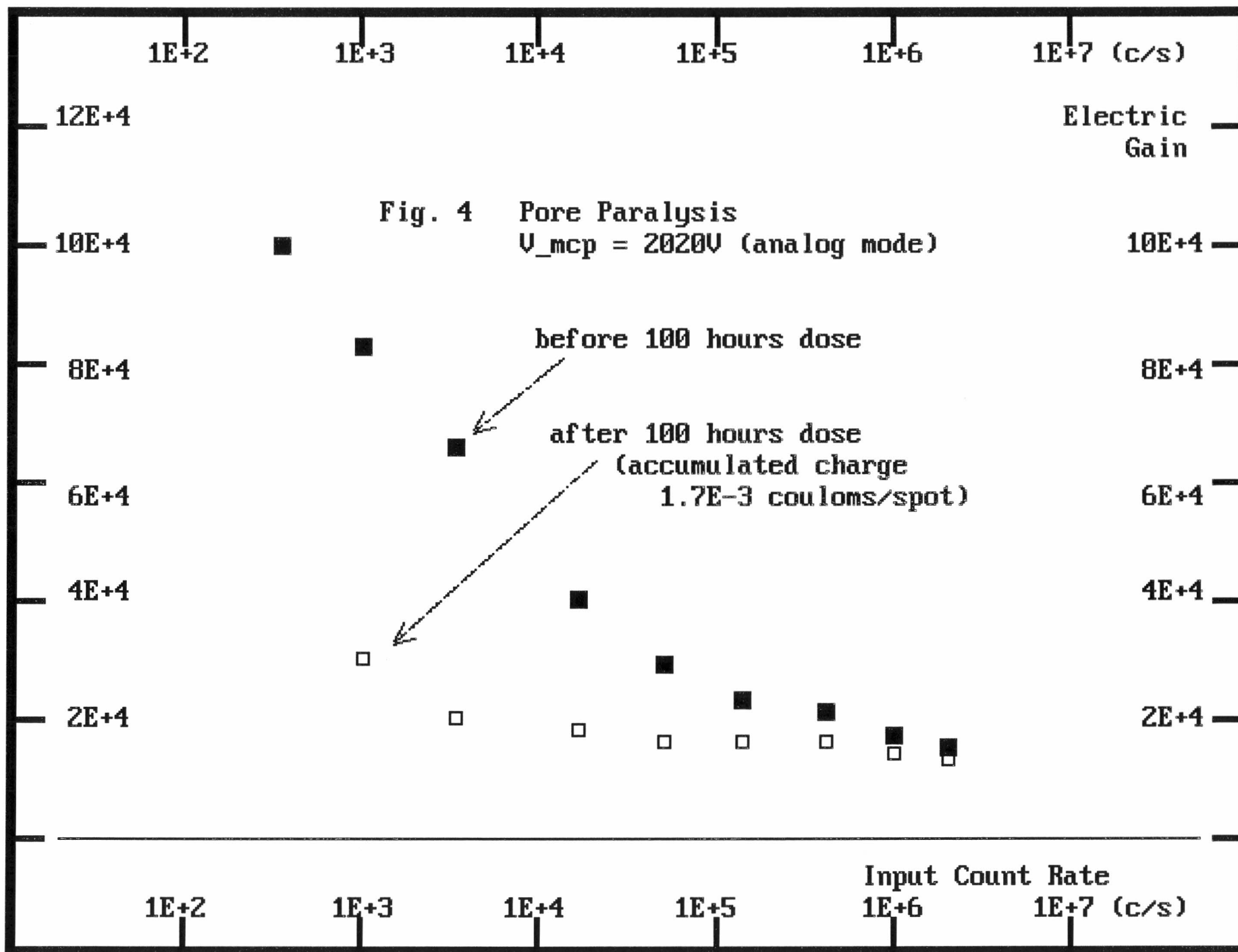


Fig. 2
Pulse height distributions for F-F input at different MCP voltages





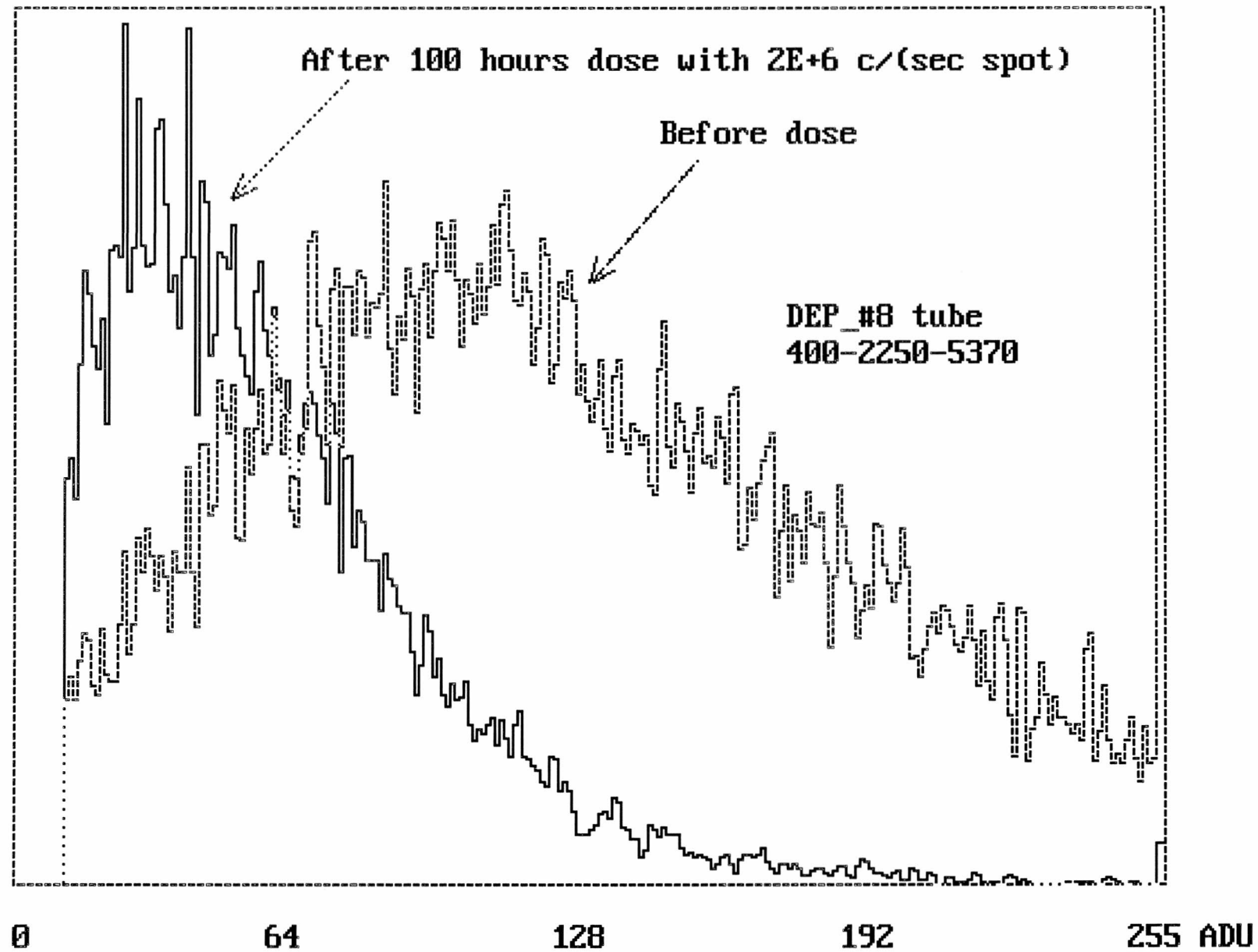
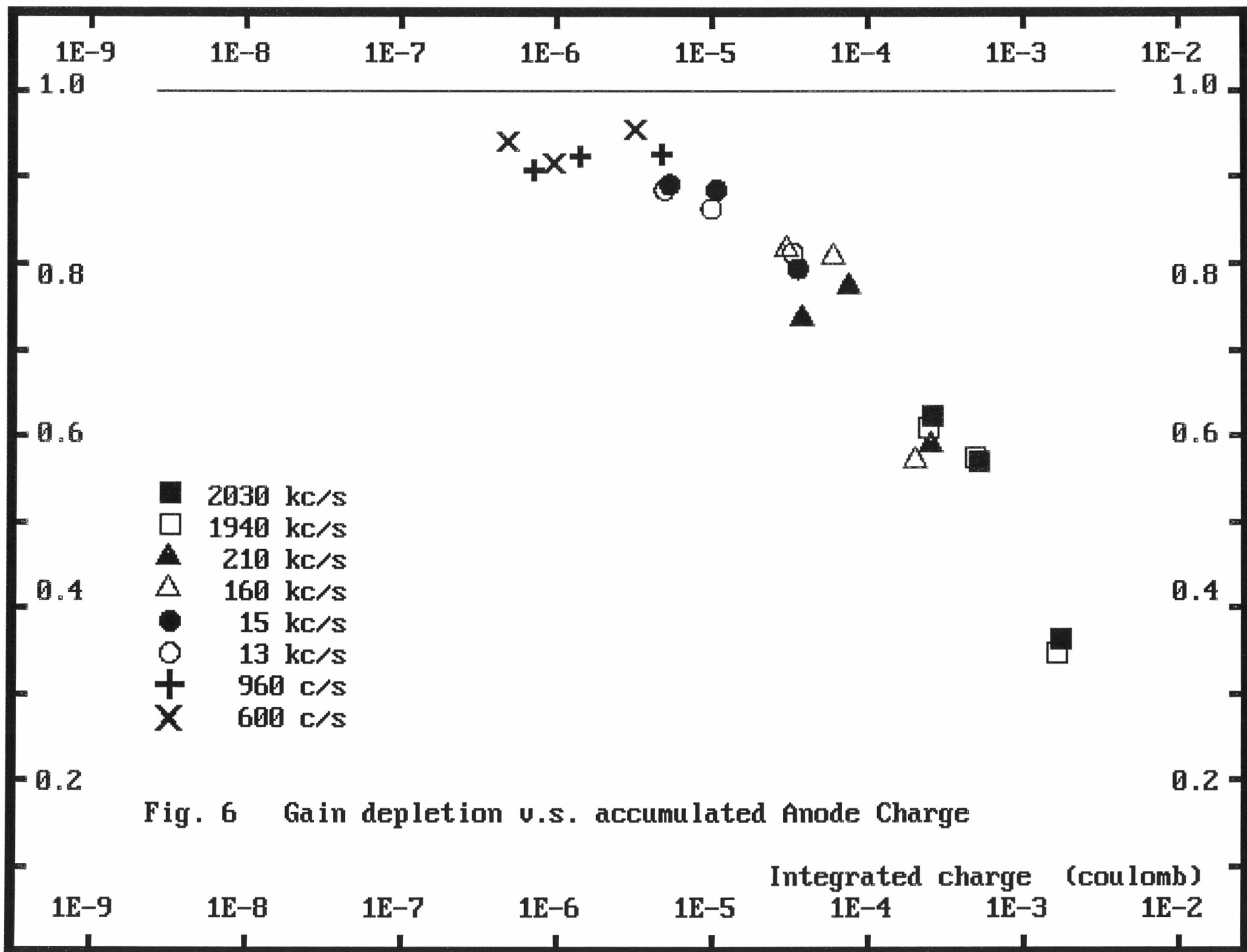
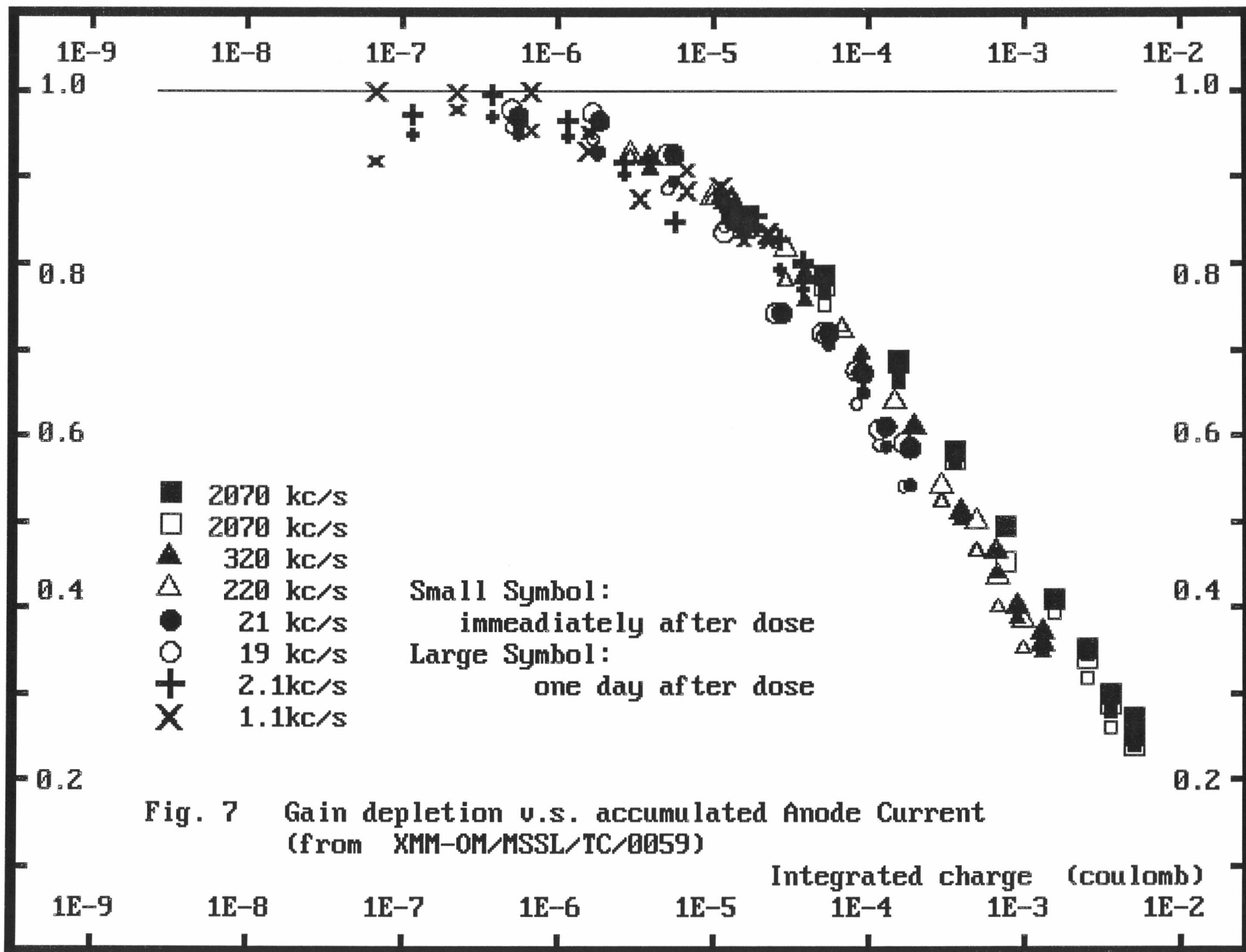


Fig. 5 Pulse height distributions by pinhole illumination





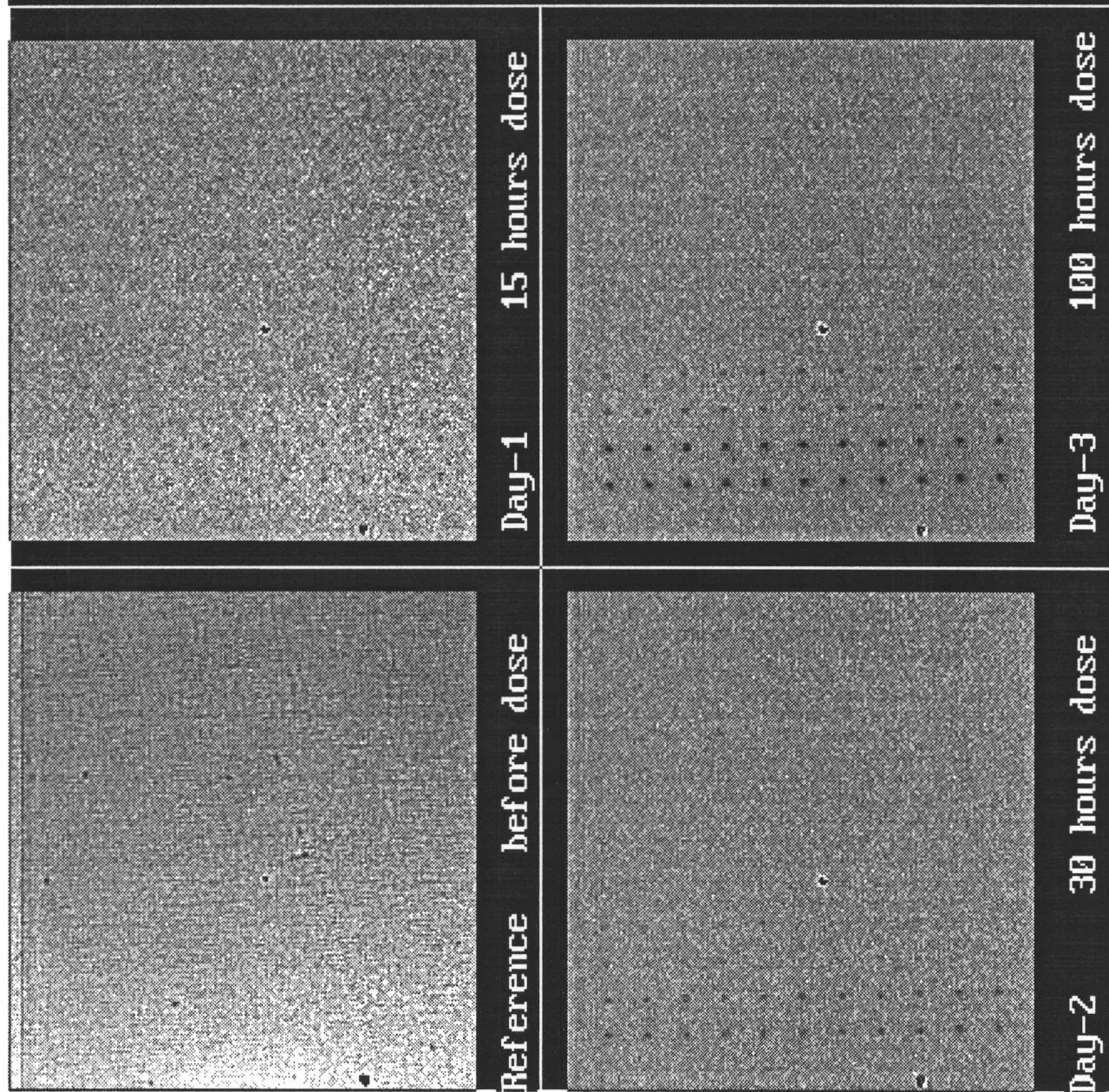


Fig. 8 High contrast F-F images during the photon dose at $V_{mcp}=2020V$

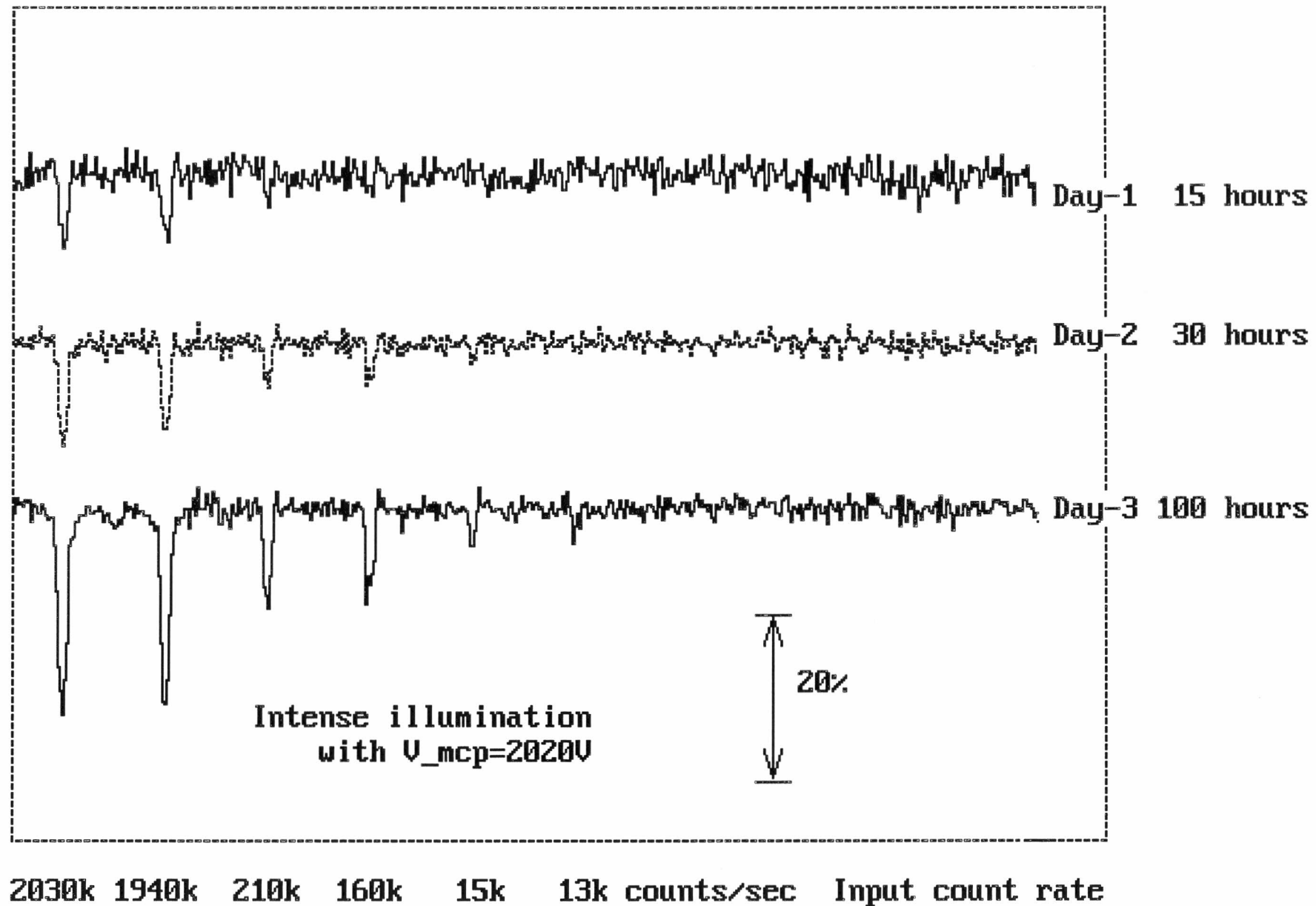


Fig. 10 Growth of sensitivity loss in blue F-F image

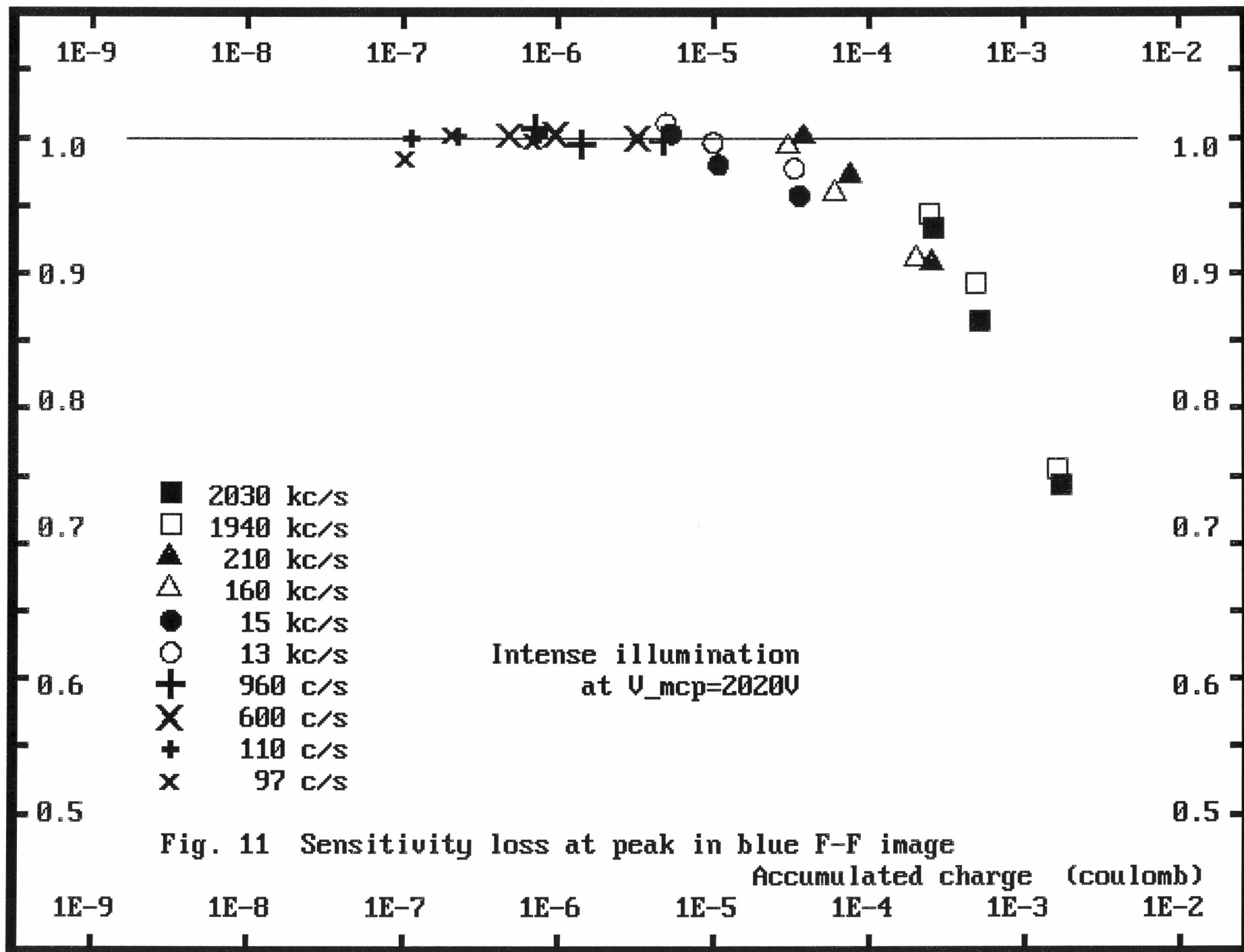


Fig. 11 Sensitivity loss at peak in blue F-F image

Accumulated charge (coulomb)

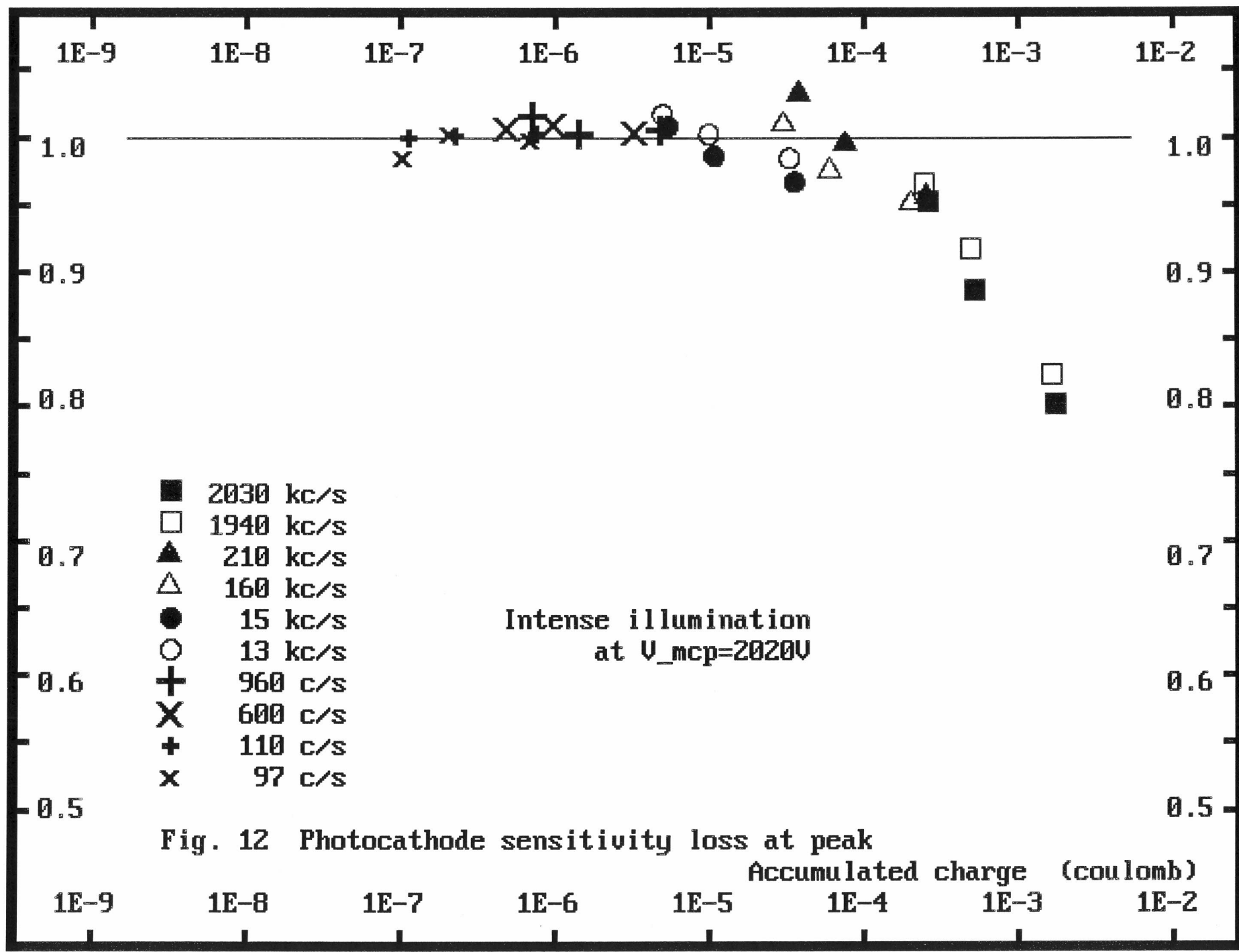
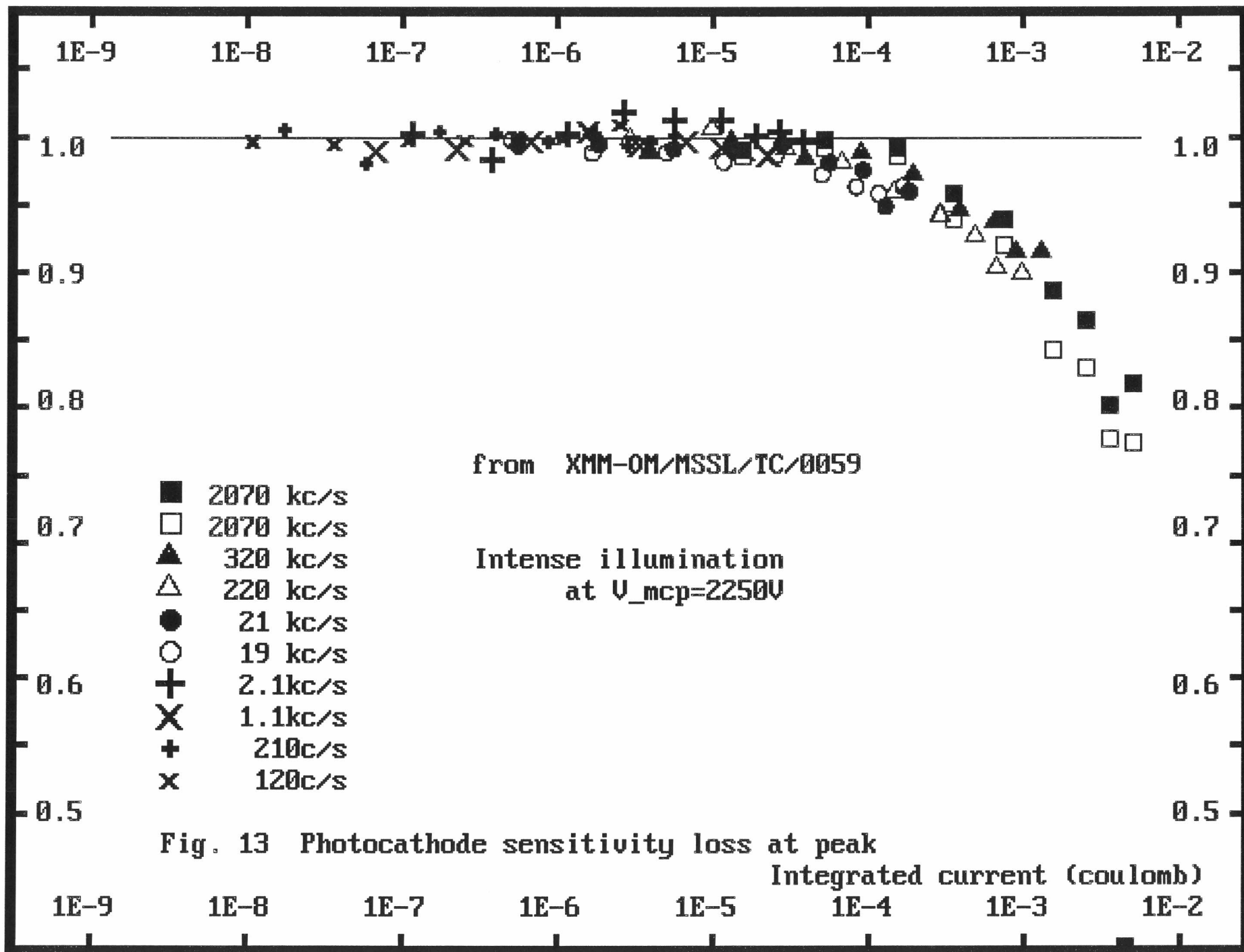
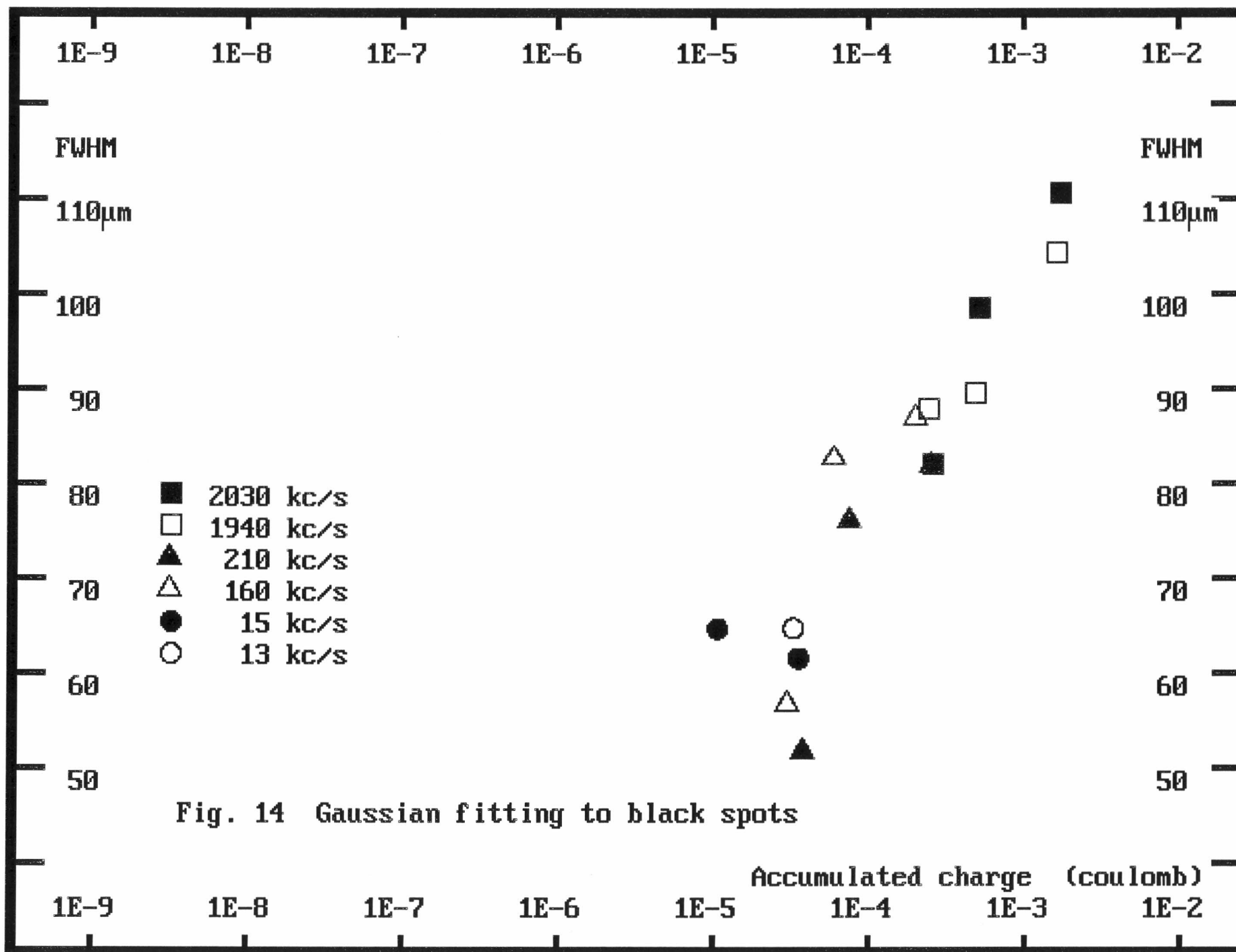


Fig. 12 Photocathode sensitivity loss at peak

Accumulated charge (coulomb)





Drk052
Drk053
Drk054
Drk055
Drk056
Drk057
Drk058
Drk059
DEP060

7200S
7200S
7200S
7200S
7200S
7200S
7200S
7200S
7200S

54000S

2000/07/04
01H 22M 13S
03H 22M 37S
05H 23M 01S
07H 23M 25S
09H 23M 49S
11H 24M 13S
13H 24M 37S
15H 25M 01S
19H 26M 24S

2000/07/05

10H 26M 48S
12H 27M 12S
15H 47M 40S

2000/07/06

09H 39M 36S

27:10

Drk061
Drk062
Ana063

7200S
7200S

30000FRs

PHD064

50000FRs